



3 1176 00115 2942

C-2

NACA

## RESEARCH MEMORANDUM

SUBSONIC AERODYNAMIC CHARACTERISTICS UP TO EXTREME ANGLES  
OF ATTACK OF AN AIRPLANE MODEL HAVING AN UNSWEPT  
WING AND A HIGH HORIZONTAL TAIL

By Bruce E. Tinling

Ames Aeronautical Laboratory  
Moffett Field, Calif.

LIBRARY COPY

FEB 4 1958

LANGLEY AERONAUTICAL LABORATORY  
LIBRARY, NACA  
LANGLEY FIELD, VIRGINIA

CLASSIFIED DOCUMENT

This material contains information affecting the National Defense of the United States within the meaning of the espionage laws, Title 18, U.S.C., Secs. 793 and 794, the transmission or revelation of which in any manner to an unauthorized person is prohibited by law.

NATIONAL ADVISORY COMMITTEE  
FOR AERONAUTICS

WASHINGTON  
February 3, 1958

UNCLASSIFIED

CLASSIFICATION CHANGED

UNCLASSIFIED

To

By author

TPA # 33 Date 10-28-60  
APK

UNCLASSIFIED

## NATIONAL ADVISORY COMMITTEE FOR AERONAUTICS

RESEARCH MEMORANDUM

SUBSONIC AERODYNAMIC CHARACTERISTICS UP TO EXTREME ANGLES  
OF ATTACK OF AN AIRPLANE MODEL HAVING AN UNSWEPT  
WING AND A HIGH HORIZONTAL TAIL

By Bruce E. Tinling

## SUMMARY

Wind-tunnel measurements of the forces and moments on a model of an airplane having pitch-up tendencies have been made at angles of attack up to  $70^\circ$ . The model had an unswept, low-aspect-ratio wing, a long fuselage, and a high horizontal tail. The tests were conducted at Mach numbers up to 0.94 at a Reynolds number of  $0.5 \times 10^6$ .

The results indicate that once the angle of attack for pitch-up is exceeded by about  $10^\circ$ , nose-up pitching moments are large, regardless of the deflection of the longitudinal control, until a stable balance point is reached at an angle of attack of  $60^\circ$  to  $70^\circ$ . Directional instability also exists for angles of attack greater than about  $20^\circ$ . Addition of tip tanks with fins delayed the pitch-up tendency for several degrees of angle of attack but did little to lessen its severity. Tests with the wing removed indicated that the fuselage vortices were of sufficient strength to cause pitch-up. However, it cannot be concluded that the fuselage vortices are the sole source of the destabilizing downwash variation for the complete airplane configuration since the wing undoubtedly alters the strength and position of the vortices.

## INTRODUCTION

Airplane configurations which employ a high horizontal tail are often subject to pitch-up at moderate to high angles of attack. Results of wind-tunnel tests of a model having this characteristic have been reported in reference 1, and an analysis of the pitch-up behavior has been presented in reference 2.

UNCLASSIFIED

The behavior of such airplane configurations at extreme angles of attack is of interest since these angles can be reached during an inadvertent pitch-up maneuver. The present investigation was initiated, therefore, to measure the forces and moments on a small-scale model of the airplane described in reference 1. Testing this small model in the relatively large test section of the Ames 12-foot pressure wind tunnel permitted angles of attack up to  $70^\circ$  to be obtained at high subsonic Mach numbers without choking the tunnel flow.

Secondary purposes of the tests were to evaluate the effects of wing-tip tanks and of tip-tank fins on the pitch-up characteristics and to obtain data with the wing removed to indicate if the vortices discharged from the fuselage are important in the pitch-up problem.

#### NOTATION

All forces and moments, with the exception of lift and drag, are referred to body axes. The longitudinal axis of the body axes system was the fuselage center line and the moment center was at the longitudinal location of the quarter point of the mean aerodynamic chord (see fig. 1). The coefficients and symbols are defined as follows:

$b$	wing span
$\bar{c}$	wing mean aerodynamic chord
$C_D$	drag coefficient, $\frac{\text{drag}}{qS}$
$C_L$	lift coefficient, $\frac{\text{lift}}{qS}$
$C_m$	pitching-moment coefficient, $\frac{\text{pitching moment}}{qS\bar{c}}$
$C_{m\text{tail}}$	increment in pitching-moment coefficient due to the tail
$C_{m\text{strakes}}$	increment in pitching-moment coefficient due to the strakes
$C_Y$	side-force coefficient, $\frac{\text{side force}}{qS}$
$C_n$	yawing-moment coefficient, $\frac{\text{yawing moment}}{qSb}$

~~CONFIDENTIAL~~

$C_l$	rolling-moment coefficient, $\frac{\text{rolling moment}}{qSb}$
$i_t$	incidence of the horizontal tail
$M$	free-stream Mach number
$q$	free-stream dynamic pressure
$R$	Reynolds number based on the wing mean aerodynamic chord
$S$	wing area
$\alpha$	angle of attack
$\beta$	angle of sideslip

#### MODEL AND APPARATUS

A drawing of the model is shown in figure 1 and pertinent geometric parameters are tabulated in table I. The model, without tip tanks, is the model designated S<sub>1</sub> in reference 3. The wings and empennage of the model were machined from high-strength steel and the fuselage from solid aluminum.

The model was sting mounted on a six-component, flexure-pivot, internal strain-gage balance. The model angle of attack could be varied from a remote station through a range of about 30°. A special sting was constructed with a knuckle which could be set in any of three positions in order to obtain the large angle range desired in the test. The angle range available with this arrangement was from -2° to 76°. A photograph of the model mounted on the sting, with the knuckle set to obtain angles of attack from 24° to 52°, is presented in figure 2(a). A close-up view of the model is shown in figure 2(b).

#### TEST PROCEDURE

The data for zero sideslip were obtained by varying the angle of the sting support for each of the sting knuckle positions. The angle-of-attack ranges for the three knuckle positions overlapped by several degrees so that the effects of changes in the interference of the large-diameter sting and of the position of the model in the air stream would be indicated by the agreement of the data taken at the same angle

CONFIDENTIAL

of attack for different knuckle positions. The sideslip angle was varied from about  $0^\circ$  to  $20^\circ$  with the model, sting, and sting support oriented to obtain constant angles of attack of approximately  $2^\circ$ ,  $13^\circ$ ,  $27^\circ$ ,  $39^\circ$ ,  $52^\circ$ , and  $64^\circ$ . The angles of attack and sideslip were determined from the known sting position with the wing off and from static calibrations of the deflection of the sting and its support under load.

The tunnel stagnation pressure was set at fairly low values during the tests to extreme angles of attack in order to keep the loads on the model and balance within safe limits. The resulting Reynolds number was  $0.5 \times 10^6$  for Mach numbers from 0.60 to 0.94. Tests at a Mach number of 0.4 to evaluate the effects of tip tanks were conducted at atmospheric pressure as a matter of convenience. The resulting Reynolds number of these tests was about  $0.9 \times 10^6$ .

Corrections to the data to take account of the effects of the tunnel walls were considered to be negligible for a model of this small size. At high angles of attack, the tail loads were undoubtedly influenced by the wake from the sting. No attempt was made to correct the data for this interference effect. The only correction applied to take account of the effects of sting interference was to adjust the axial-force measurement to correspond to that for a model having free-stream static pressure on its base.

## RESULTS AND DISCUSSION

### Longitudinal and Lateral-Directional Characteristics up to Extreme Angles of Attack

The results of the measurements of the longitudinal forces and moments to extreme angles of attack are presented in figure 3. The trends of these results are the same regardless of Mach number up to the highest test Mach number of 0.94. It is evident that the pitch-up tendency began at about  $15^\circ$  angle of attack, and is attributable to a destabilizing variation of downwash with angle of attack. As the angle of attack for pitch-up was exceeded, the effectiveness of the tail as a longitudinal control was reduced markedly, indicating the tail to be in the wing wake. Once the angle of attack for pitch-up was exceeded by more than about  $10^\circ$ , a nose-up pitching moment existed for the most positive tail incidence available ( $i_t = 5^\circ$ ) until extreme angles of attack were reached. The tail regained effectiveness as a stabilizer at an angle of attack of about  $45^\circ$ . The control effectiveness at this angle, however, approached zero because of the high angle of attack of the tail. A stable balance point was reached when the angle of attack reached between  $60^\circ$  and  $70^\circ$ . The maximum pitching-moment coefficient contributed by the horizontal tail at these extreme angles of attack

was between -0.5 and -0.6 which corresponds to a tail normal-force coefficient, based on tail area, of between 1.0 and 1.2.

It should be noted that the test Reynolds number based on the component of velocity normal to the fuselage center line and the fuselage diameter was less than the critical value for flow normal to a circular cylinder. Under full-scale conditions, this Reynolds number would be greater than the critical value for a circular cylinder when the angle of attack exceeds a moderate value. If the crossflow on the fuselage forebody approximates that for a circular cylinder, it would be expected that the fuselage crossflow drag coefficient, and therefore the destabilizing pitching-moment coefficient contributed by the fuselage, would be less under full-scale conditions than during the wind-tunnel tests. Therefore, the maximum tail loads and the angle of attack at which the stable balance point occurs could be smaller under full-scale conditions than the values indicated by the wind-tunnel test results.

Results of tests to determine the effects of large angles of attack on the side force and on the rolling, yawing, and pitching moments due to sideslip are presented in figure 4. These results indicate that at angles of attack of  $27^\circ$  and greater the lateral coefficients are not zero at zero sideslip and are not symmetrical about zero sideslip. This lack of lateral symmetry undoubtedly arises from asymmetrical stall patterns resulting from slight inaccuracies in model construction. At an angle of attack of  $26.9^\circ$ , the model was directionally unstable and had a large adverse variation of rolling moment with sideslip angle near zero sideslip. At higher angles of attack, the model was generally directionally unstable. This instability is to be expected since the vertical tail is in the wake of the wing and of the fuselage in this angle-of-attack range.

#### Effects of Wing-Tip Tanks and of Tip-Tank Fins

The effects of adding several wing-tip-tank-fin combinations on the lift and pitching-moment characteristics are shown in figure 5. The lift coefficient at which a pitch-up tendency appears was increased by about 0.15 when tip tanks with fins were added to the configuration. It is obvious that some of the improvement was a direct result of the increase in lift due to adding the tanks. Some increase in the angle of attack for pitch-up was also realized, however. The sources of the improvement are illustrated in figure 6. Adding the tip tanks alone did not change the variation of the pitching moment of the wing-fuselage combination with angle of attack, but did result in a more favorable downwash variation as the angle of attack was increased beyond  $8^\circ$  (see variation of  $C_{m_{tail}}$  with angle of attack in fig. 6). The tip-tank fins, on the other hand, did not influence the tail loads but contributed a small stabilizing pitching moment to the wing-fuselage combination at angles of attack

greater than about  $12^\circ$ . The improvement arising from both of these effects is, unfortunately, small in comparison with that required to prevent pitch-up of this airplane configuration.

#### Longitudinal Characteristics of the Fuselage-Tail Combination

Tests were made with the wing removed to indicate if the downwash field resulting from the fuselage vortices is important in the pitch-up problem. The results of these tests are presented in figure 7 and indicate that the downwash from the fuselage vortex system caused the tail to be destabilizing for angles of attack greater than  $16^\circ$  to  $18^\circ$ . The change in the contribution of the tail to the pitching-moment curve slope  $dC_m/d\alpha$  as the angle of attack is increased from zero is shown in figure 8. These results indicate the same trends in the tail contribution to  $dC_m/d\alpha$  whether the wing is on or off. It cannot be concluded from this, however, that the fuselage vortices are the sole source of the destabilizing downwash variation since the presence of the wing undoubtedly alters their strength and position. Evidence of the influence of the wing on the destabilizing tail moments contributed by the fuselage vortices is furnished by the results of tests with strakes attached to the sides of the fuselage. These surfaces were horizontal projections of about  $3/16$  of an inch and extended along the midline of the fuselage from the nose to the fairing which corresponds to the duct entry. As might be expected, the strakes caused the pitch-up to be more severe by both increasing the nose-up pitching moment of the fuselage and by increasing the destabilizing contribution of the tail at high angles of attack. At angles of attack greater than about  $12^\circ$ , however, the influence of the strakes on the tail pitching moments was much smaller for the complete configuration than for the fuselage-tail combination (see fig. 9).

Tests were also made with only one strake attached to the fuselage in the hope of establishing an asymmetrical flow pattern which would be less detrimental to the longitudinal stability. This result was not realized and the single strake caused the pitch-up to be somewhat more severe.

#### CONCLUSIONS

Wind-tunnel tests to measure the characteristics of a small-scale model of an airplane having strong pitch-up tendencies have indicated the following:

1. Once the angle of attack for pitch-up was exceeded by about  $10^\circ$ , nose-up pitching moments existed regardless of the deflection of the longitudinal control until a balance point was reached at angles of attack of  $60^\circ$  to  $70^\circ$ .

2. Addition of wing-tip tanks with horizontal fins delayed the pitch-up tendency to slightly higher angles of attack, and effected a small reduction in the longitudinal instability at higher angles of attack.

3. Tests of the model with the wing removed indicate that the fuselage vortices are of sufficient strength to cause pitch-up. It cannot be concluded, however, that the fuselage vortices are the sole source of the destabilizing variation of downwash for the complete airplane configuration since the wing undoubtedly alters their strength and position.

Ames Aeronautical Laboratory  
National Advisory Committee for Aeronautics  
Moffett Field, Calif., Nov. 5, 1957

#### REFERENCES

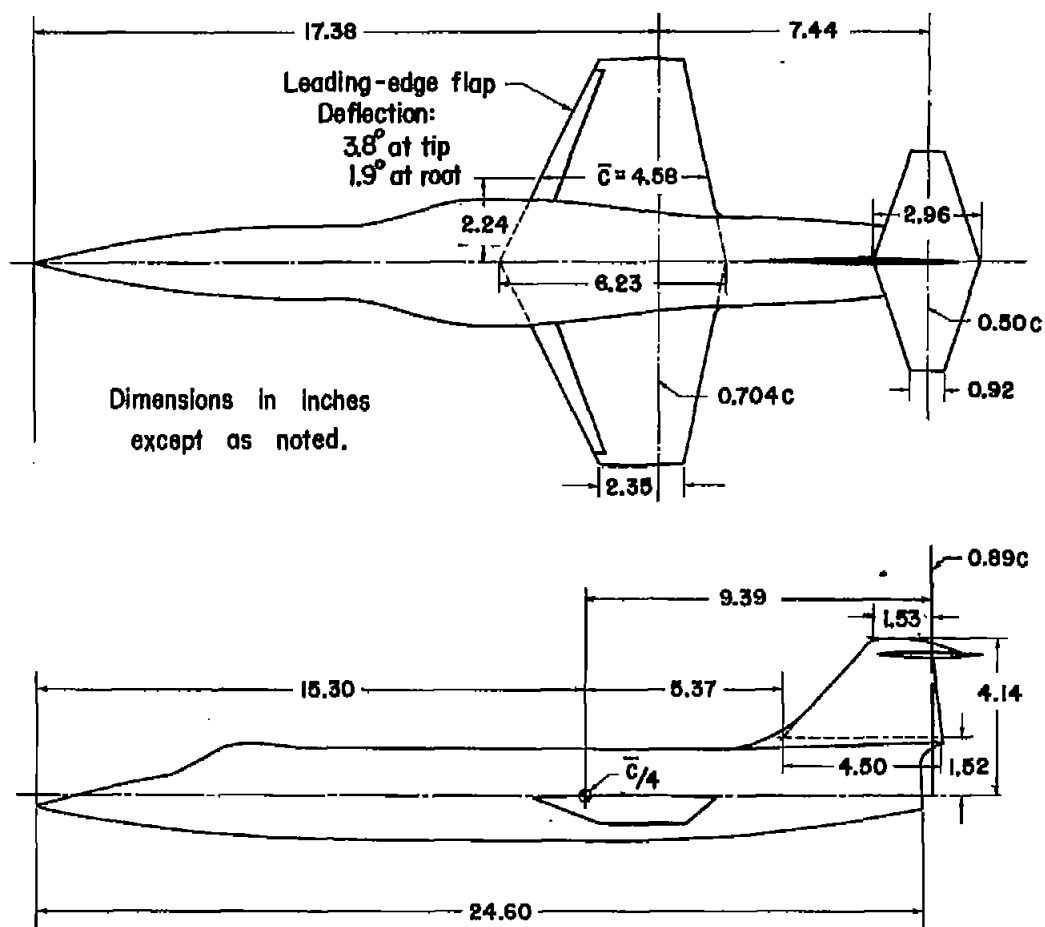
1. Buell, Donald A., Reed, Verlin D., and Lopez, Armando E.: The Static and Dynamic-Rotary Stability Derivatives at Subsonic Speeds of an Airplane Model With an Unswept Wing and a High Horizontal Tail. NACA RM A56IO4, 1956.
2. Sadoff, Melvin A., and Stewart, John D.: An Analytical Evaluation of the Effects of an Aerodynamic Modification and of Stability Augmenters on the Pitch-up Behavior and Probable Pilot Opinion of Two Current Fighter Airplanes. NACA RM A57K07, 1958.
3. Summers, James L., Treon, Stuart L., and Graham, Lawrence A.: Wind-Tunnel Investigation at Mach Numbers From 0.8 to 1.4 of Static Longitudinal and Lateral-Directional Characteristics of an Unswept-Wing Airplane Model. NACA RM A56E22, 1956.



TABLE I.- GEOMETRY OF THE MODEL

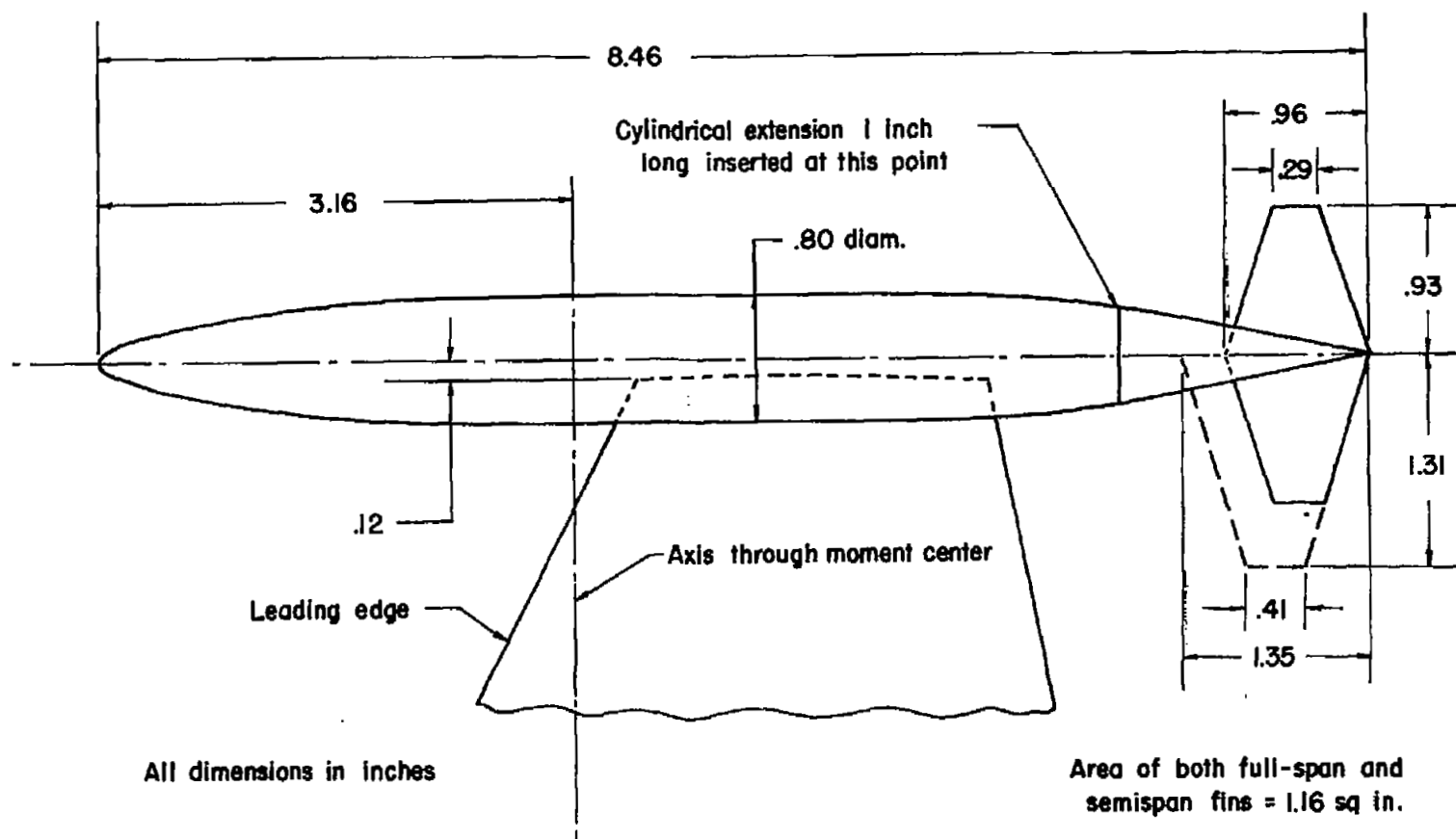
<b>Wing</b>	
Airfoil section (forward 0.5c elliptical, aft 0.5c circular arc)	
Thickness ratio, percent c . . . . .	3.4
Area, horizontal projection including the portion within the body, sq in. . . . .	45.16
Mean aerodynamic chord, in. . . . .	4.58
Span, in. . . . .	10.53
Aspect ratio . . . . .	2.45
Taper ratio . . . . .	0.38
Sweep of quarter-chord line in plane of wing, deg . . . . .	18.2
Unswapt element, percent c . . . . .	70.4
Dihedral, deg . . . . .	-10
Leading-edge flaps	
Area, sq in. . . . .	3.72
Chord, percent c . . . . .	14.6
Deflection, deg . . . . .	
Root . . . . .	1.9
Tip . . . . .	3.8
<b>Horizontal tail</b>	
Airfoil section (forward 0.5c elliptical, aft 0.5c circular arc)	
Root thickness ratio, percent c . . . . .	4.9
Tip thickness ratio, percent, c . . . . .	2.6
Area, sq in. . . . .	11.09
Mean aerodynamic chord . . . . .	2.12
Span, in. . . . .	5.72
Aspect ratio . . . . .	2.95
Taper ratio . . . . .	0.31
Sweep of quarter-chord line, deg . . . . .	10.1
Unswapt element, percent c . . . . .	50
Incidence, deg . . . . .	0
Dihedral, deg . . . . .	0
<b>Vertical tail</b>	
Airfoil section (forward 0.5c elliptical, aft 0.5c circular arc)	
Root thickness ratio, percent c . . . . .	4.3
Tip thickness ratio, percent c . . . . .	5.0
Area, exposed, sq in. . . . .	8.06
Mean aerodynamic chord . . . . .	3.44
Aspect ratio . . . . .	0.87
Taper ratio . . . . .	0.46
Sweep of quarter-chord line, deg . . . . .	35
Unswapt element, percent c . . . . .	89.3

Refer to Table I for  
model specifications.



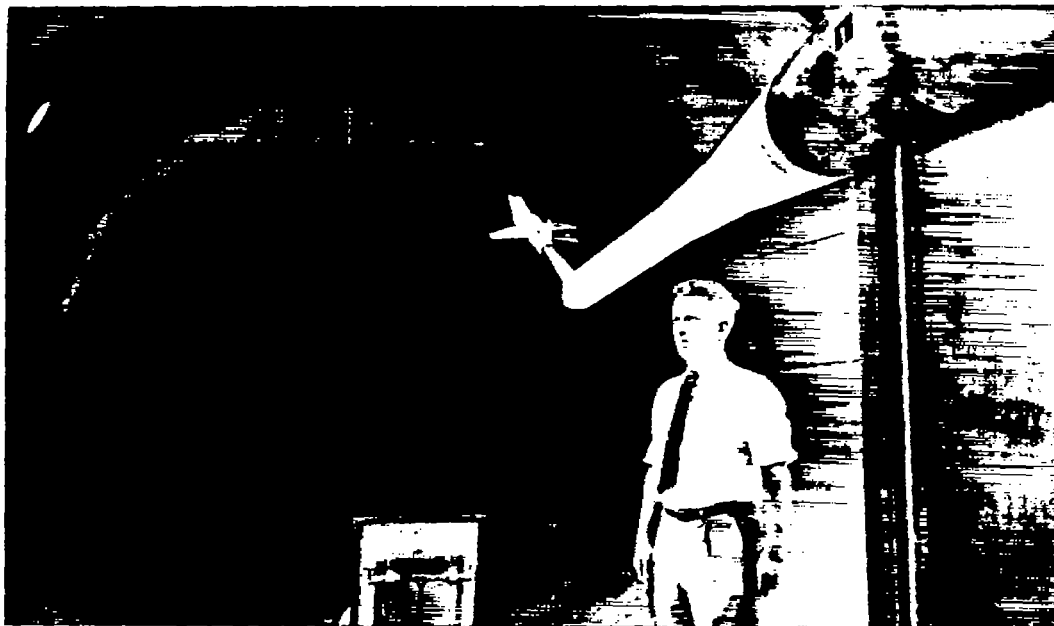
(a) Basic model.

Figure 1.- Geometry of the model.



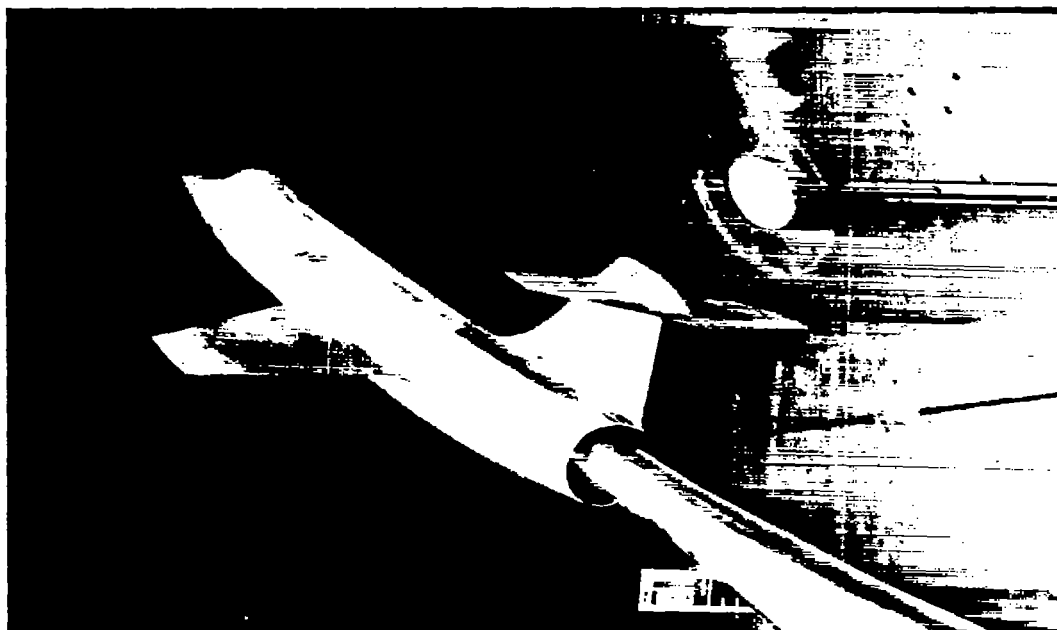
(b) Tip-tank details.

Figure 1. - Concluded.



A-22423

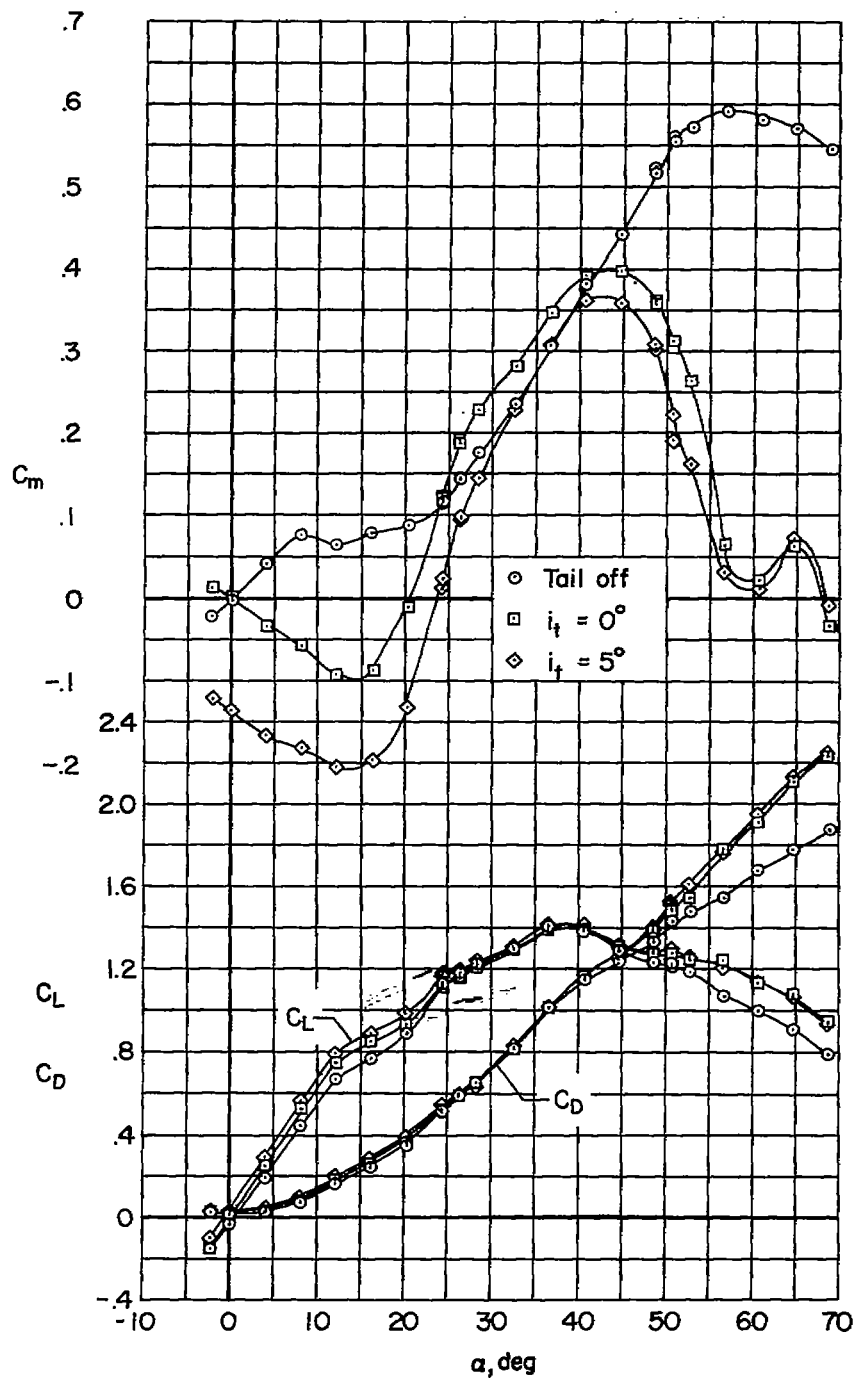
(a) Rear view showing the sting-support arrangement with the sting knuckle set to obtain an angle-of-attack range from  $24^\circ$  to  $52^\circ$ .



A-22424

(b) Close-up view of model.

Figure 2.- Photographs of the model mounted in the wind tunnel.

(a)  $M = 0.60$ Figure 3.- Lift, drag, and pitching-moment characteristics;  $R = 0.5 \times 10^6$ .

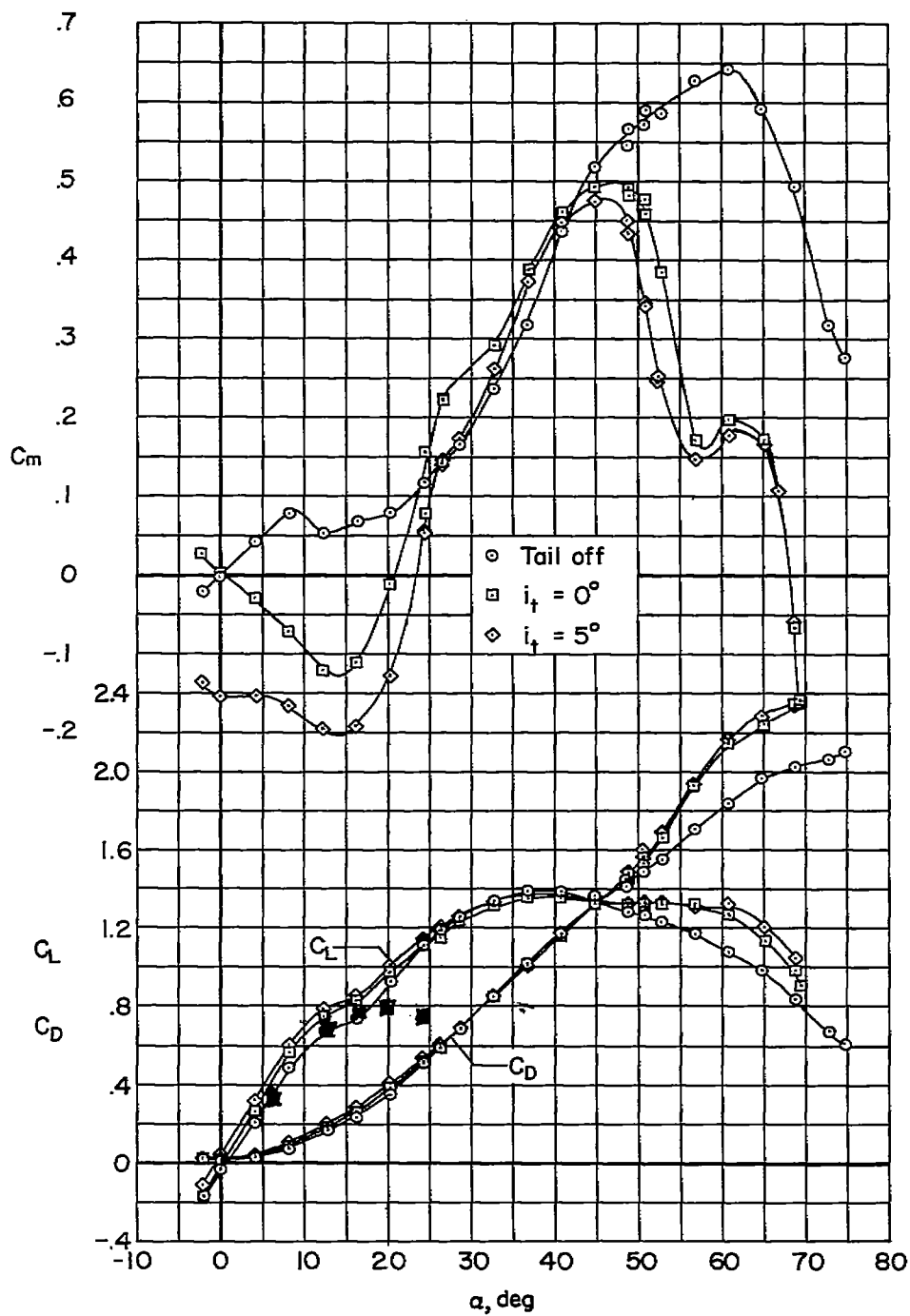
(b)  $M = 0.80$ 

Figure 3.- Continued.

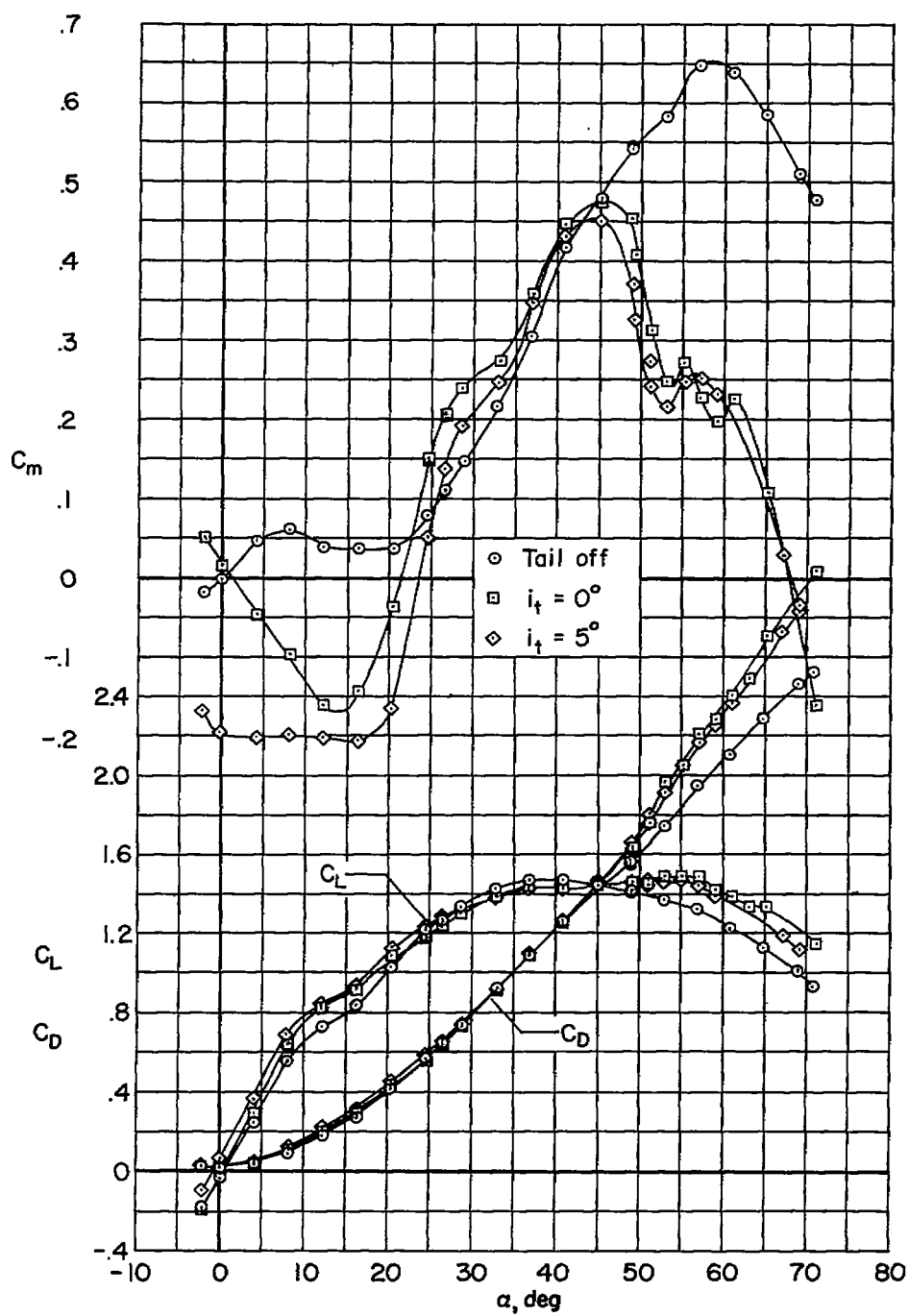
(c)  $M = 0.90$ 

Figure 3.- Continued.

~~CONFIDENTIAL~~

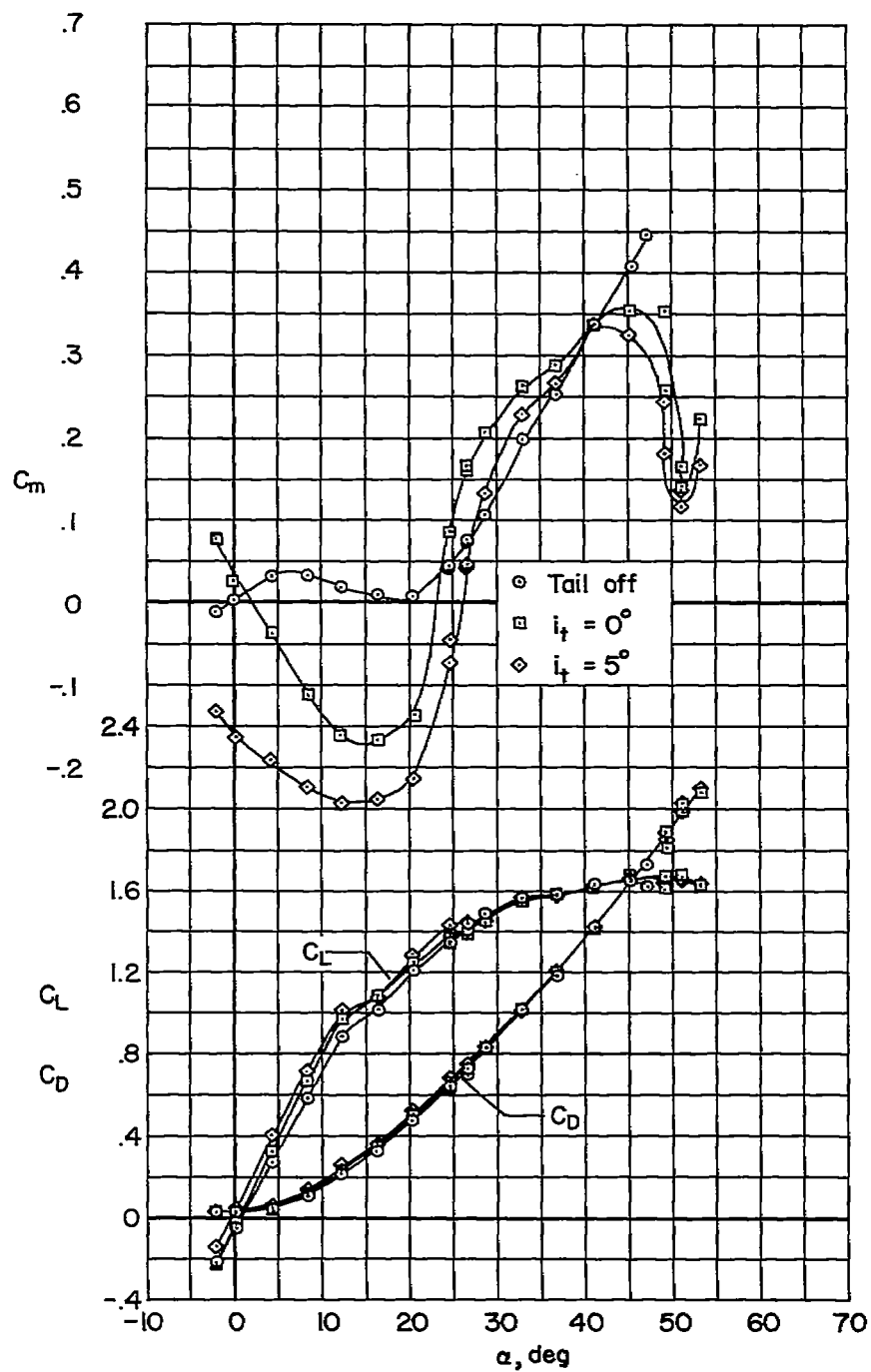
(a)  $M = 0.94$ 

Figure 3.- Concluded.

CONFIDENTIAL



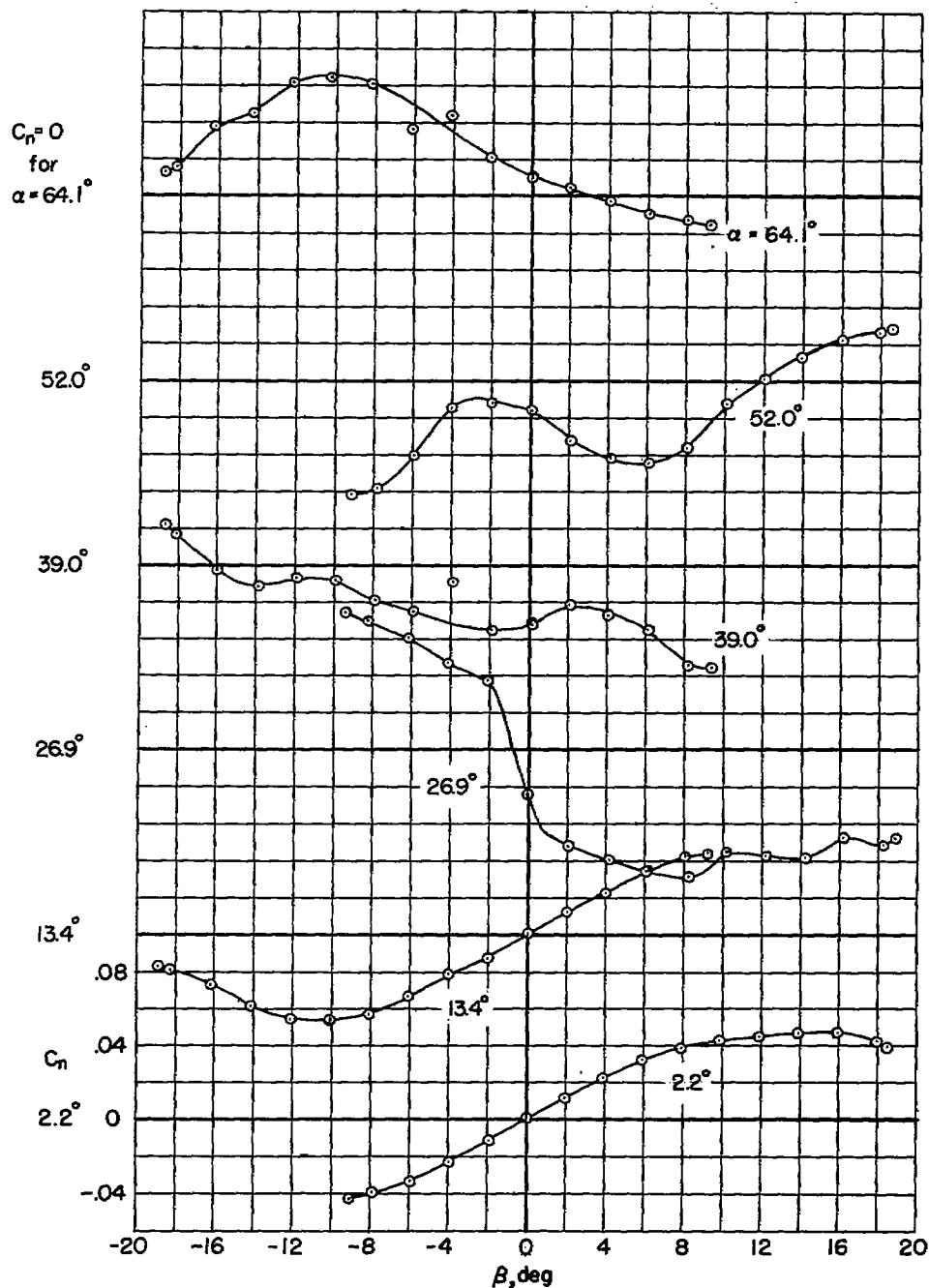
(a)  $C_n$  vs.  $\beta$ 

Figure 4.- The variation of side force and of rolling-moment, yawing-moment, and pitching-moment coefficients with sideslip;  $M = 0.80$ ,  $R = 0.5 \times 10^6$ .

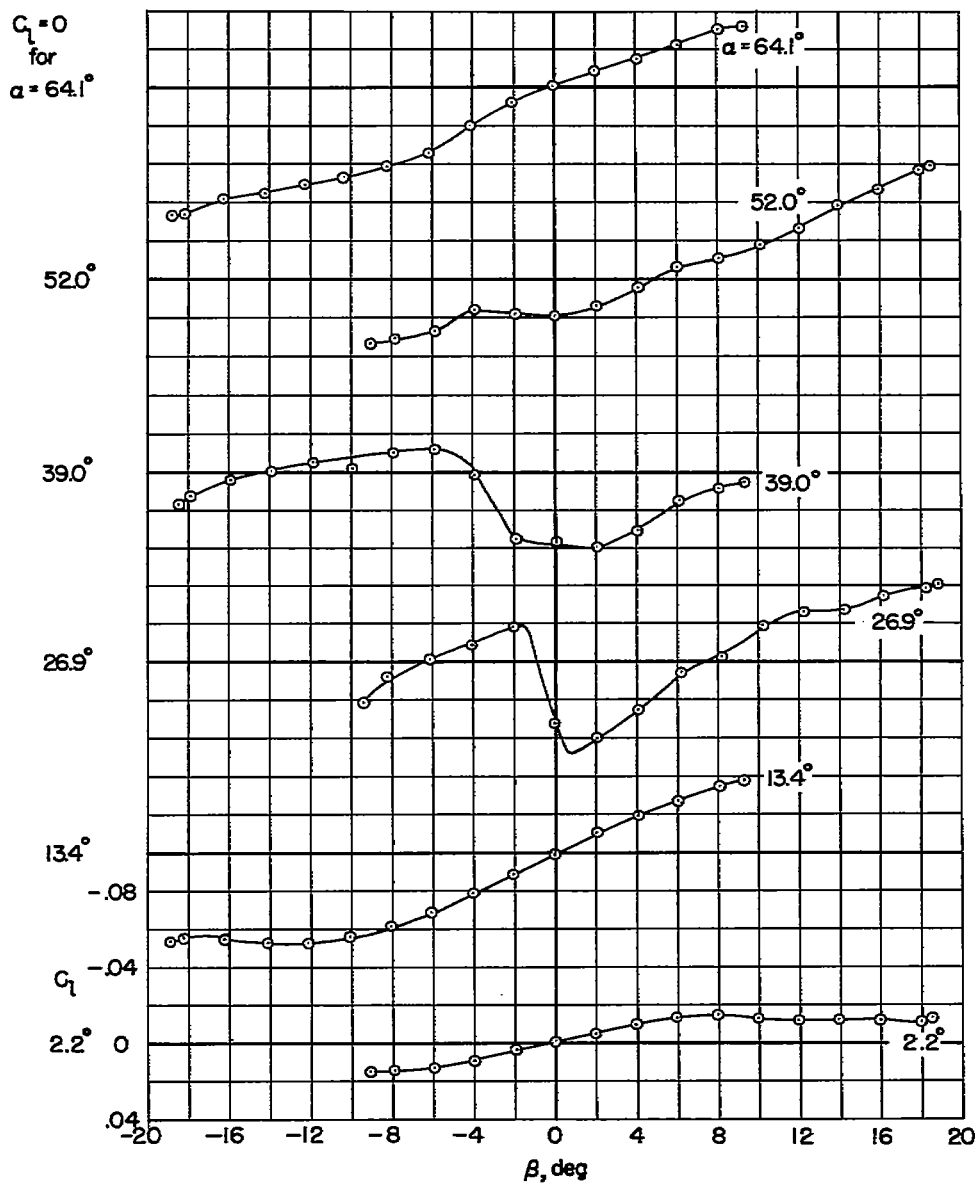
(b)  $C_L$  vs.  $\beta$ 

Figure 4.- Continued.

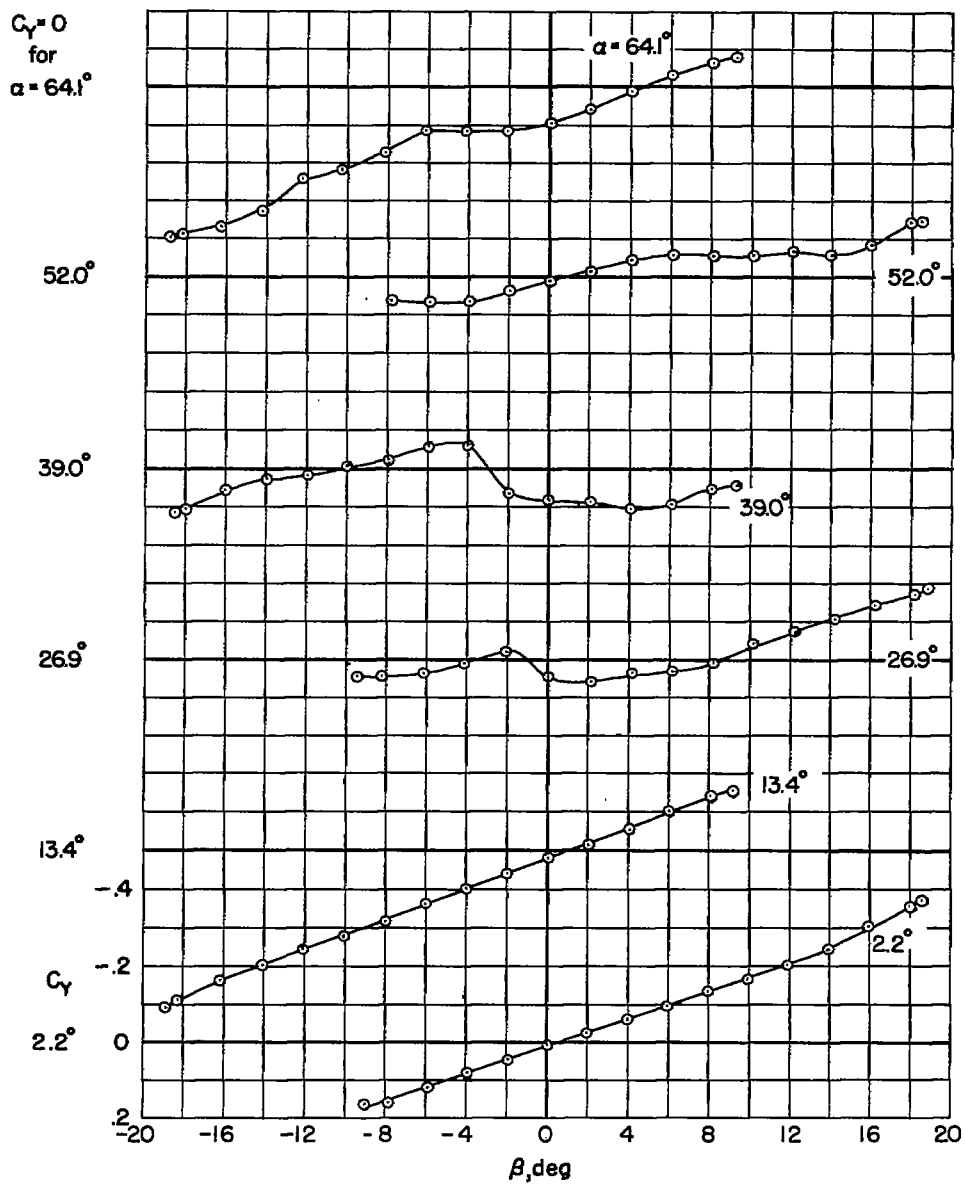
(c)  $C_Y$  vs.  $\beta$ 

Figure 4.- Continued.

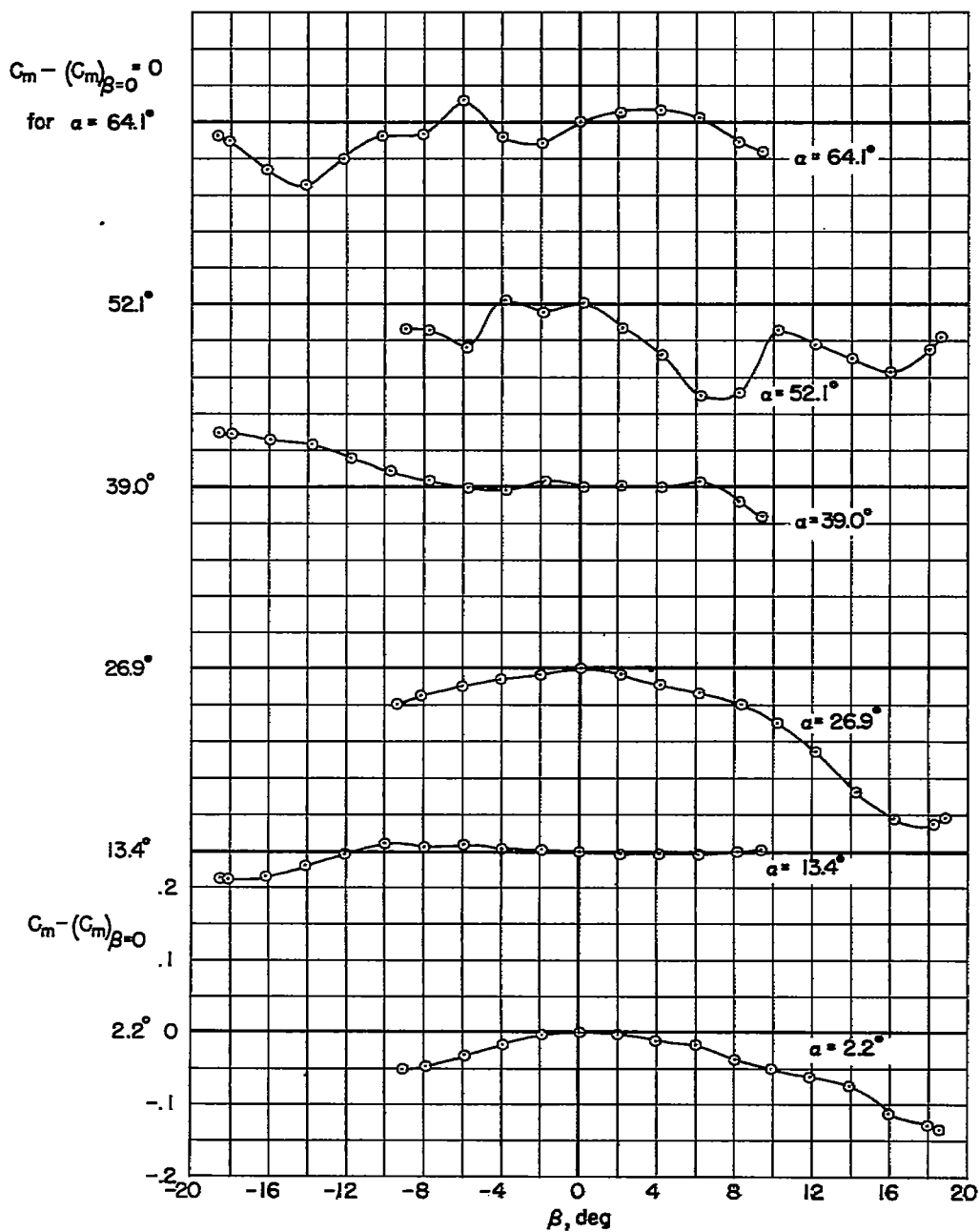
(d)  $C_m - (C_m)_{\beta=0}$  vs.  $\beta$ 

Figure 4.- Concluded.

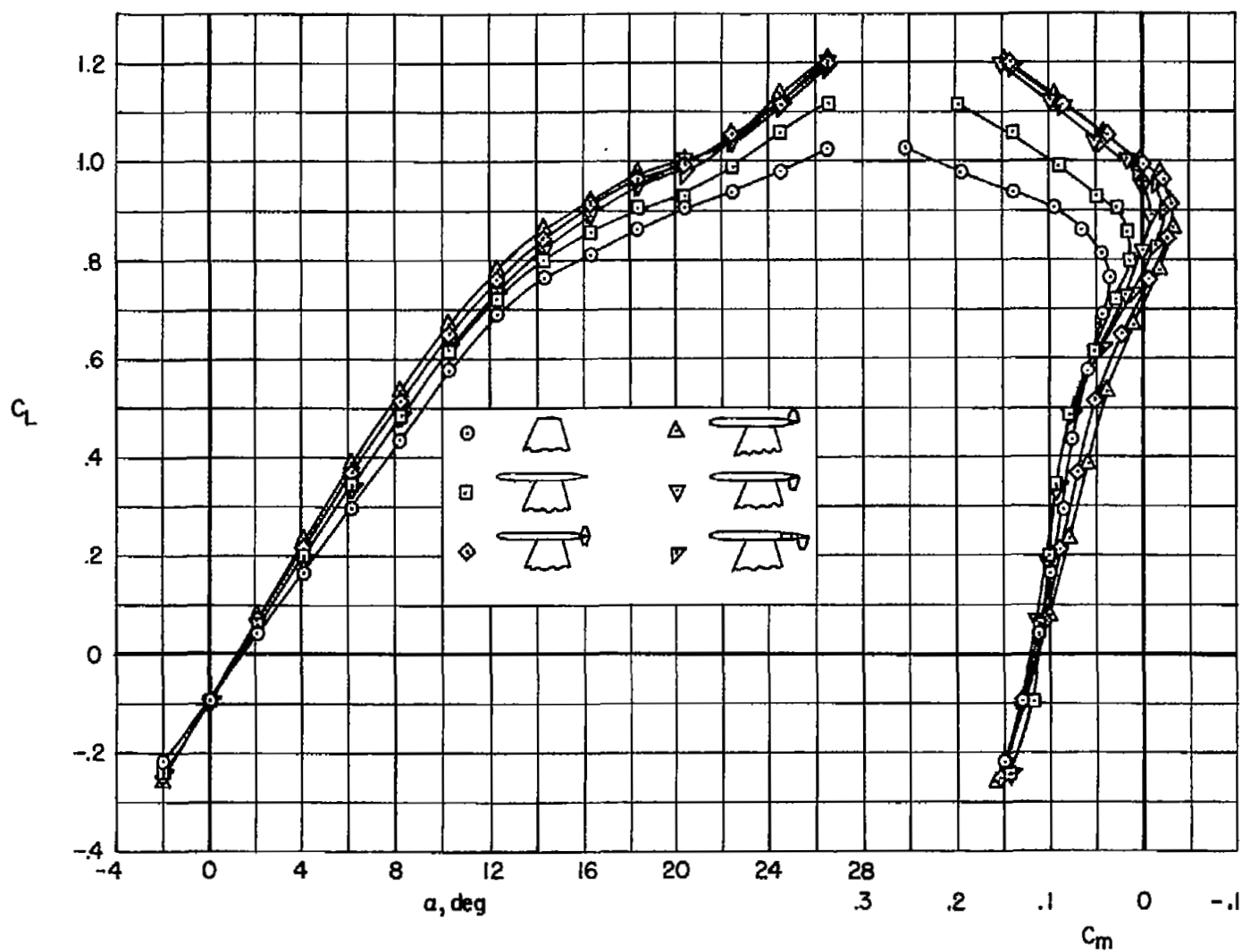


Figure 5.- The effects of several tip-tank fin arrangements on the low-speed lift and pitching-moment characteristics;  $M = 0.40$ ,  $R = 0.9 \times 10^6$ ,  $i_t = -5^\circ$ .

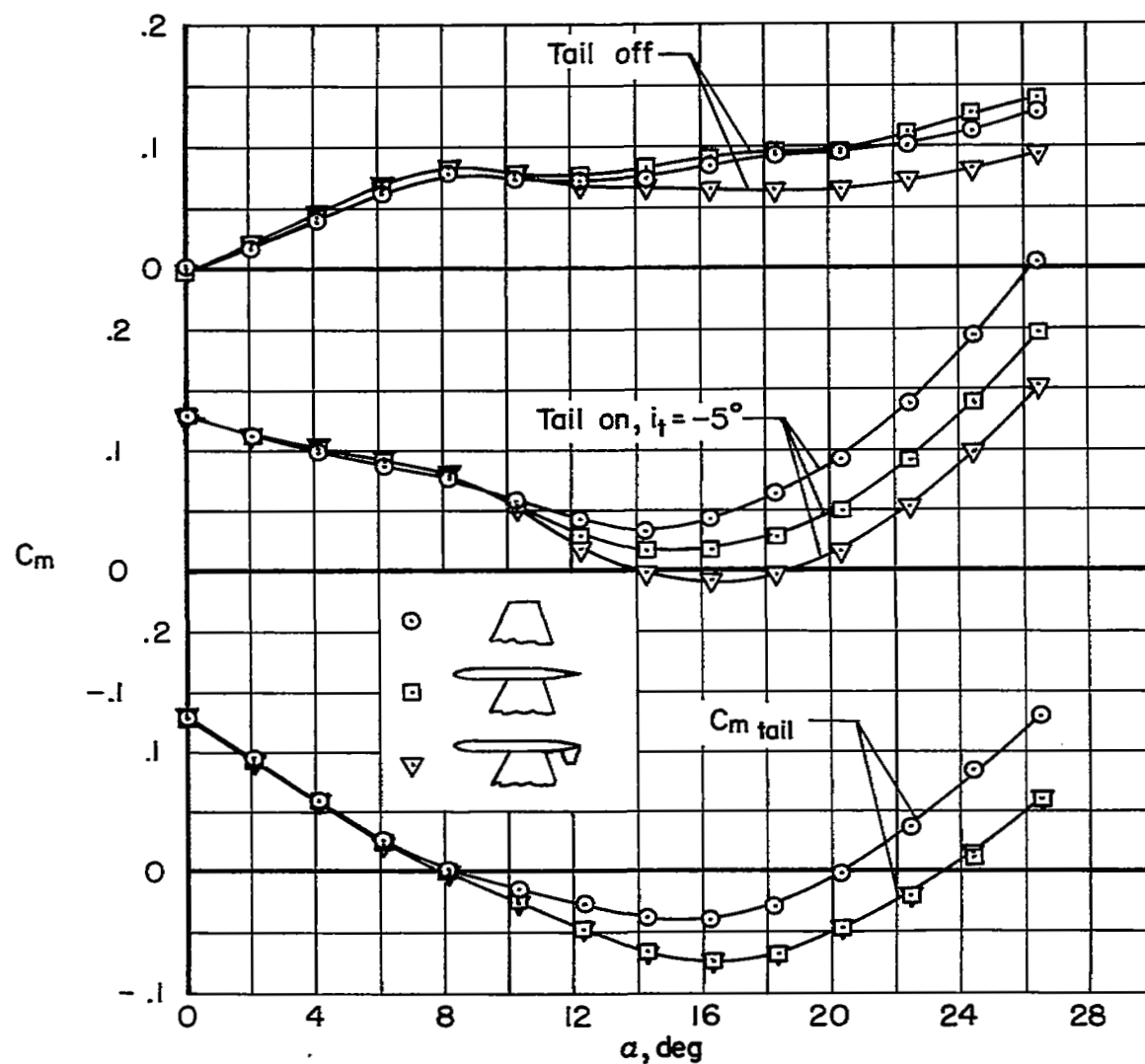


Figure 6.- Effects of adding tip tanks and tip-tank fins on the pitching-moment characteristics and on the pitching moment contributed by the horizontal tail;  $M = 0.4$ ,  $R = 0.9 \times 10^6$ .

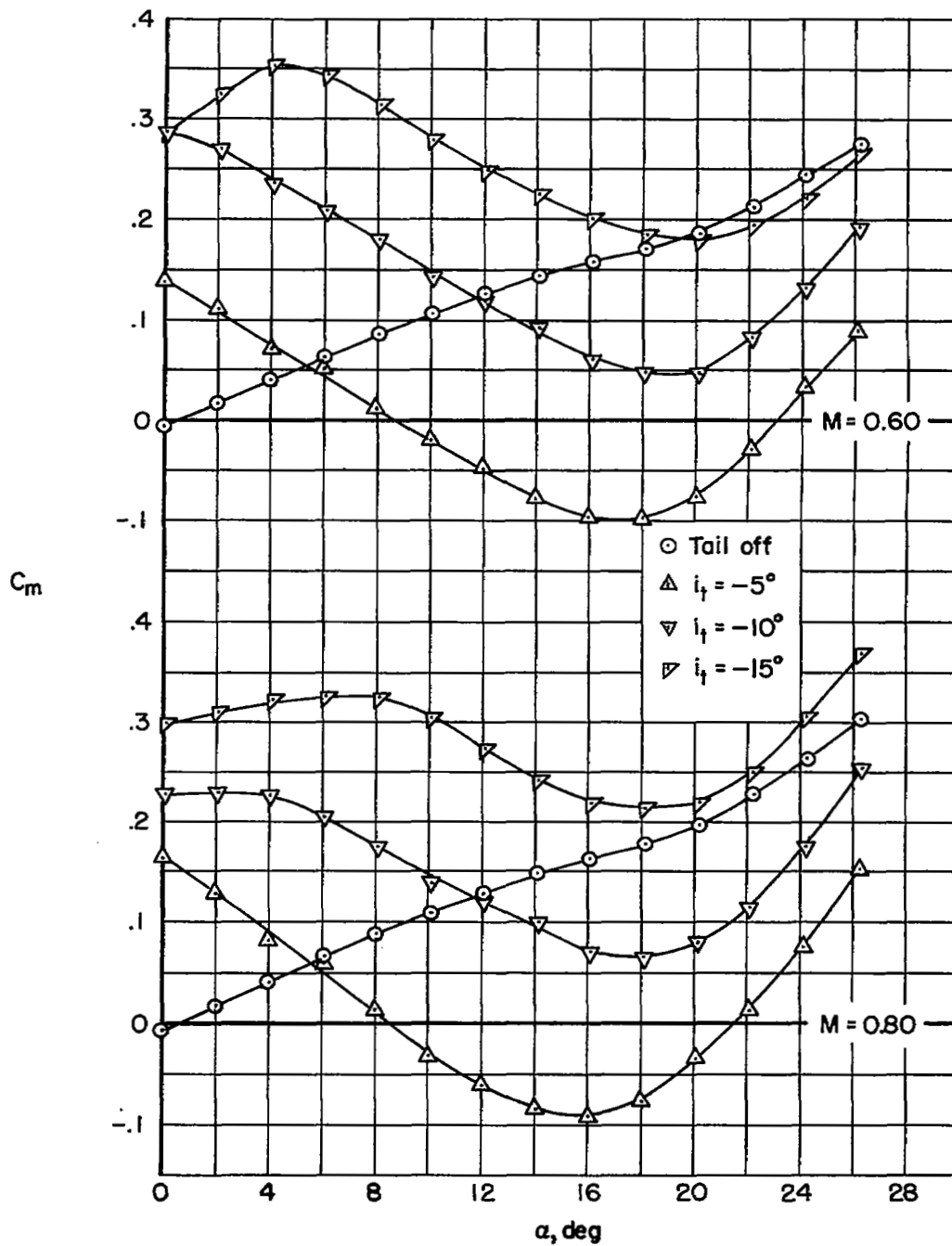
(a)  $M = 0.60$  and  $0.80$ 

Figure 7.- The pitching-moment characteristics of the fuselage-tail combination;  $R = 0.5 \times 10^6$ .

~~CONFIDENTIAL~~

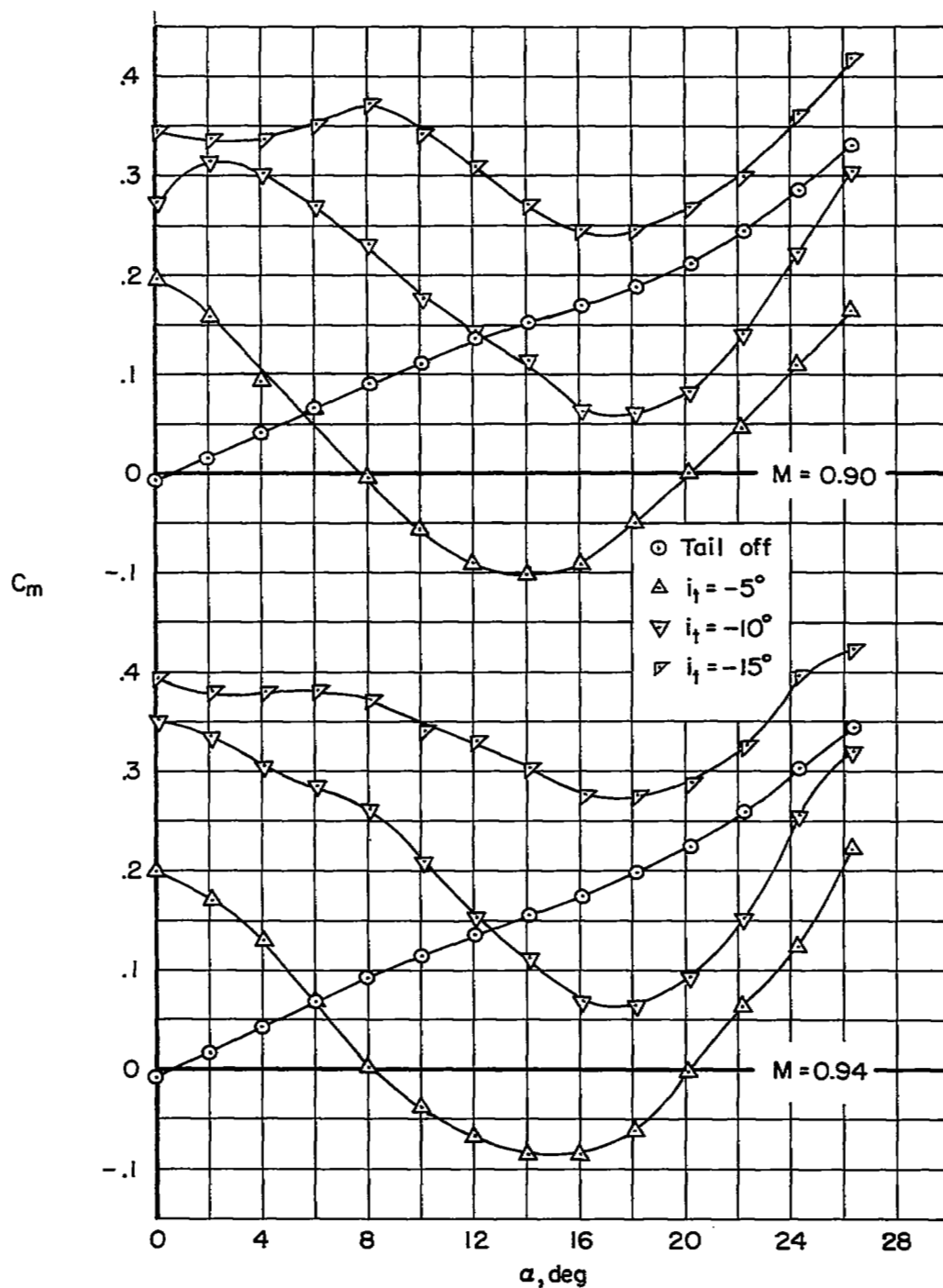
(b)  $M = 0.90$  and  $0.94$ 

Figure 7.- Concluded.



$$\left(\frac{dC_m}{d\alpha}\right)_{\text{tail}} - \left[\left(\frac{dC_m}{d\alpha}\right)_{\text{tail}}\right]_{\alpha=0} = 0$$

for

$$M = 0.60$$

$$\left(\frac{dC_m}{d\alpha}\right)_{\text{tail}} - \left[\left(\frac{dC_m}{d\alpha}\right)_{\text{tail}}\right]_{\alpha=0}$$

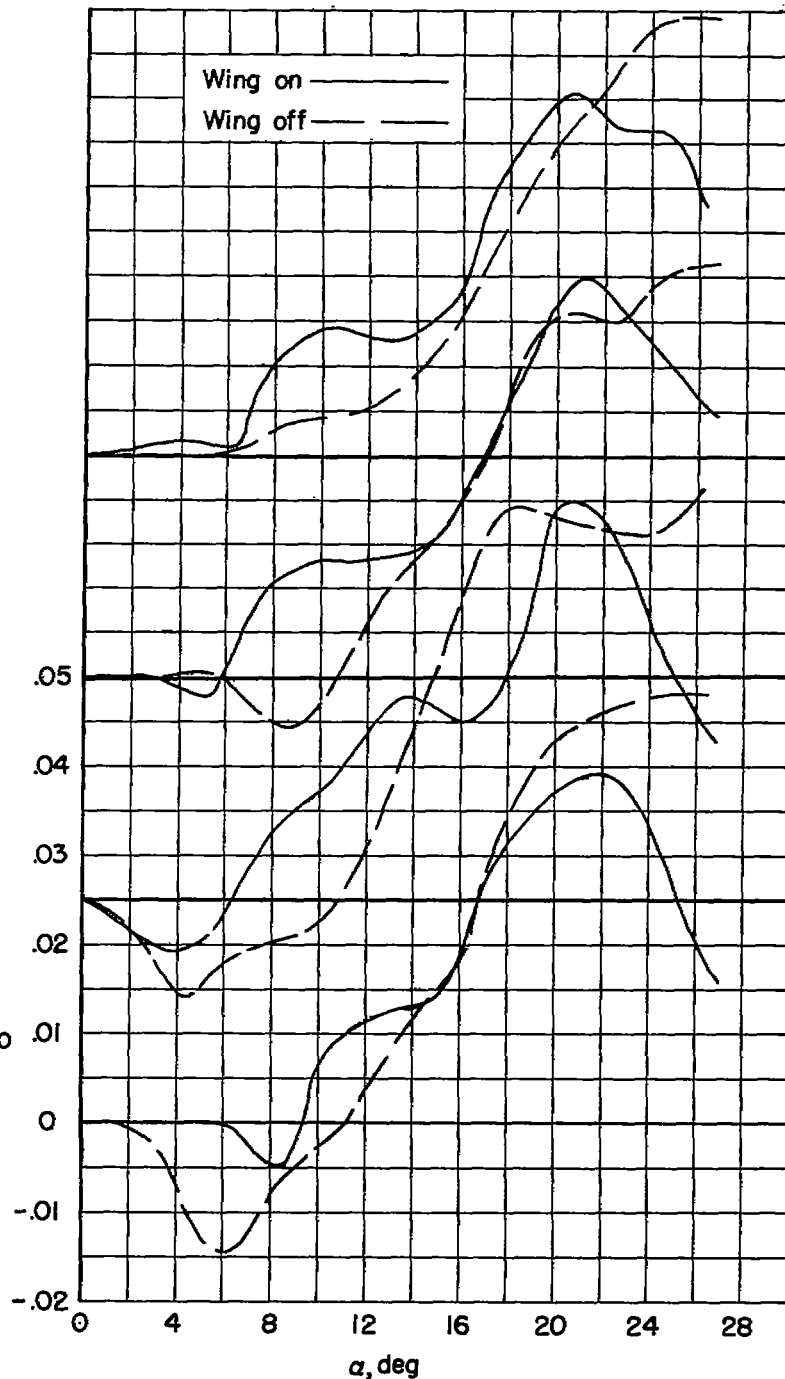


Figure 8.- The variation with angle of attack of the contribution of the tail to  $dC_m/d\alpha$  with the wing on and with the wing off;  $R = 0.5 \times 10^8$ ,  $i_t = -5^\circ$ .

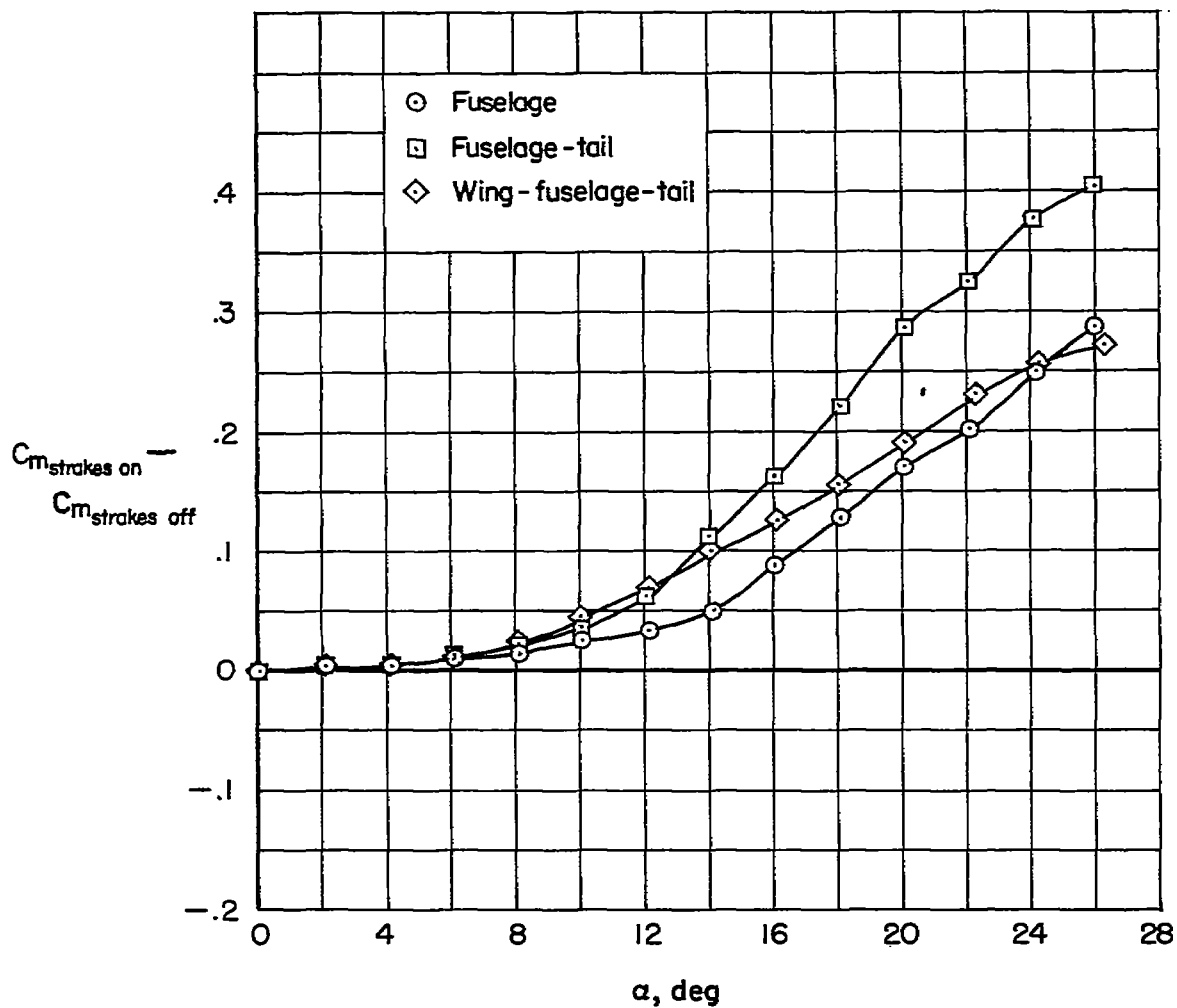


Figure 9.- The pitching-moment contribution of fuselage strakes with the wing on and with the wing off;  $M = 0.40$ ,  $R = 0.9 \times 10^6$ .